Temporal Estimation of Snow Line Altitude in Glaciers of the Southern Patagonian Icefield Using Google Earth Engine

Ignacio Ortiz Diaz [1], María Gabriela Lenzano [1], Diego Araneo [2]

[1] Lab. de Geomática Andina, Instituto Argentino de Nivología, Glaciología y Ciencias Ambientales (IANIGLA)-Centro Científico Tecnológico (CCT), CONICET-Mendoza CP 5500, Argentina - (irortiz, mlenzano)@mendoza-conicet.gob.ar
[2] Programa Regional de Meteorología, Instituto Argentino de Nivología, Glaciología y Ciencias Ambientales (IANIGLA)-Centro Científico Tecnológico (CCT), CONICET-Mendoza CP 5500, Argentina - daraneo@mendoza-conicet.gob.ar

Keywords: Snow line, equilibrium line altitude, Google Earth Engine, image segmentation, infrared bands

Abstract

The study analyzes the variability over time of the Snow Line Altitude (SLA) and its correspondence with the Equilibrium Line Altitude (ELA) in four glaciers of the Southern Patagonian Icefield (SPI): Perito Moreno, Upsala, Viedma and De los Tres. Using Google Earth Engine and Landsat satellite imagery, an automated algorithm based on the Otsu image segmentation method was developed to analyze the 1985-2023 time series to obtain the Snow Cover Ratio (SCR) and subsequently estimate the SLA using the ALOS World 3D DSM. The study employed the near infrared (NIR) and shortwave infrared (SWIR) bands of Landsat images, with the SCR and subsequently the SLA determined using only the NIR band, as well as a band ratio between the NIR/SWIR bands. The results indicated that the Viedma glacier showed a statistically significant positive trend in SLA elevation, while the other three glaciers showed a stationary behavior with high variability. The SLA calculated using the NIR/SWIR bands tended to be higher compared to the NIR band calculation, especially for the Viedma and Upsala glaciers. Comparisons with previous studies (De Angelis, 2014; Popovnin et al., 1999) and recent glaciological measurements from the Inventario Nacional de Glaciares (2015-2022) showed that the SLA derived from the NIR bands aligned more closely with the aforementioned works.

1. Introduction

Glaciers worldwide have been undergoing profound changes, mainly in their geometry and volume due to the influence of climate change (Jacob et al., 2012; Bamber et al., 2018; Zemp et al., 2019). Glaciers in the Patagonian Andes showing one of the highest rates of retreat and thinning in the Southern Hemisphere in recent times (Rivera et al., 2008, 2012; Moragues et al., 2018; Mouginot & Rignot, 2015; Dussaillant et al., 2019; Lenzano et al., 2023). The Equilibrium Line Altitude or ELA is frequently used as indicator to assess the balance of glaciers with respect to climate (Zemp et al., 2007; De Angelis, 2014; Ohmura & Boettcher, 2022). The ELA can be approximated as the Snow Line Altitude (SLA) during the final stages of the ablation season (Meier, 1962). On the other hand, Google Earth Engine (GEE) is a platform that provides satellite image collections with medium to high spatial, spectral and temporal resolutions, which are open access and also has an integrated development environment-IDE (Tamiminia et al., 2020). This enables the direct processing of geospatial data, including the estimation of snow cover ratio (SCR) and subsequent the estimation of the SLA (Li et al., 2022), in cloud-based environments.

The goal of this study is to test an algorithm within the GEE platform to obtain an automated time series (1985-2023) of the SLA of Perito Moreno, Upsala, Viedma and De los Tres glaciers. In order to achieve the objective, we employ the automatic segmentation of Landsat images using the methodology proposed by Otsu, (1979), which is based on the near-infrared (NIR) and shortwave infrared (SWIR) bands. The glaciers under study, whose main characteristics are outlined in Table 1, are located in the Southern Patagonian Icefield (Fig. 1) and representing the largest continental ice mass in South America (Bown et al., 2019). The processing follows the guidelines proposed by the World Meteorological Organization (WMO) by considering the SLA as a zone within the glacier instead of a line. The results obtained were compared with previous works of estimation of the SLA from approaches similar to this study (De Angelis, 2014) and glaciological measurements (Popovnin et al., 1999; work carried out by the Inventario Nacional de Glaciares 2015-2023).

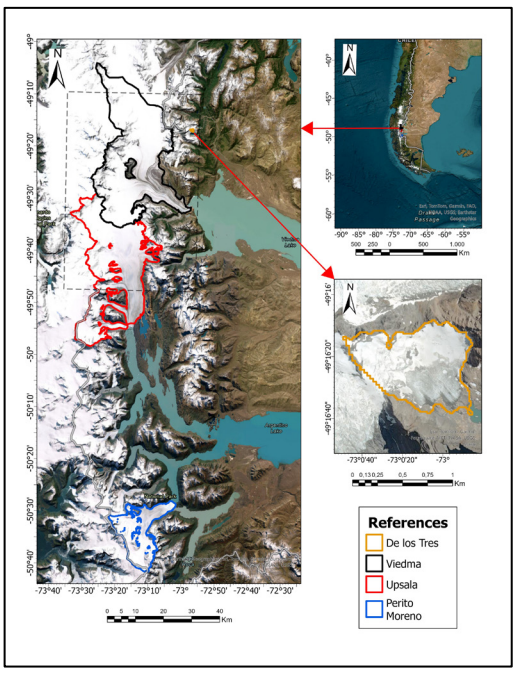

Figure 1. Study area. The grey and dashed lines represent the border limits between Chile and Argentina, on which we do not set precedents. Basemap: EsriMap (ArcGISPro)

Glacier	Long.	Lat.	Area (Km^2) *	Max (m.a.s.l)	Min (m.a.s.l)
Perito Moreno	73,2°W	50,2°S	259	2834	175
Upsala	73,3°W	49,9°S	883	3261	327
Viedma	73,3°W	49,4°S	974	3470	342
De Los Tres	73,0°W	49,3°S	0.73	1853	1228

Table 1. Main geographic characteristics of the studied glaciers. * Data extracted from Lannutti et al., (2024) for the Perito Moreno, Upsala and Viedma glaciers; and from the World Glacier Monitoring Service -WGMS (https://wgms.ch/data-exploration/) for De los Tres glacier.

The Otsu method was selected for two principal reasons. Initially, it has already been employed by other researchers in ice/snow segmentation studies (Rastner et al., 2019; Li et al., 2022; Macfee, 2023, references which are included in the present study). The second reason is the simplicity of implementation when assembling the code within the Google Earth Engine Code Editor, which facilitates more straightforward automation.

2. Data and Methods

2.1 Satellite Imagery

Google Earth Engine has a satellite product catalogue of several petabytes of information, among which all the Landsat missions launched to date are available (Pham-Duc et al., 2023). We worked with Landsat 5 TM (LT05), Landsat 7 ETM+ (LE07) and Landsat 8 OLI/TIRS (LC08) collections, which are atmospherically and geometrically corrected to land surface reflectance in the GEE data catalog. The bands used to obtain the ice/snow differentiation were the Near Infrared (NIR, band 4 for LT05-LE07 and band 5 for LC08), the Shortwave Infrared (SWIR1, band 5 for LT05-LE07 and band 6 for LC08) and the Quality Assessment (QA) band calculated by the United States Geological Survey (USGS), and contained information regarding cloud cover, cloud shadows, cirrus and other data. The spatial resolution of all bands is 30 meters.

2.2 Digital Elevation Model (DSM)

The ALOS World 3D 30 m Digital Surface Model (DSM AW3D30), which is also part of the GEE data catalog, contains a 30-meter horizontal resolution elevation band. The DSM was generated from the 5 m resolution obtained by stereoscopic mapping of optical images (Takaku et al., 2020). Following Macfee (2023), this DSM was chosen due to its precise vertical accuracy of approximately 8.33 meters (Bettiol et al., 2021).

2.3 Snow Line Analysis in Earth Engine

The algorithm used in GEE is a modification of the one developed by Li et al., (2022) and Macfee, (2023). In order to identify the Landsat images that could be utilized in GEE, it was necessary to consider those images taken at the end of the ablation season (between February 1st and April 15th) for each year of study (1985-2023). In addition, the images included have a minimum of 65% cloud-free area. A modification of the CFMask algorithm, which employs the quality assessment (QA) band of the images, was utilized to mask clouds and their shadows in the images that met the aforementioned conditions. Rastner et al., (2019) and Li et al., (2022) considered that to calculate the SLA for a given year, at least three images should be available, thereby selecting the SLA that is at the highest altitude. Due to the persistent presence of cloud cover in the region, numerous years of the time series were unable to achieve this condition. Accordingly, a year with a single image comprising cloud cover of less than 35% of the glacier surface is deemed valid. This resulted in a subsequent statistical analysis, the details will be provided subsequently.

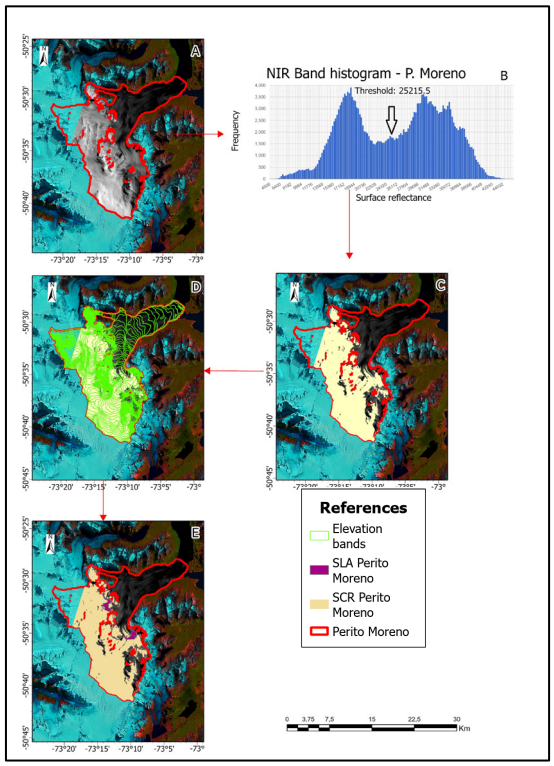

Figure 2. Application of the Otsu segmentation on the Perito Moreno glacier: A) NIR band over which the segmentation will be performed. B) Frequency histogram of surface reflectance values of the NIR band, where the threshold value that distinguishes ice and snow can be observed. C) Estimation of the SCR using the threshold value. D) Intersection between the SCR and the elevation bands. E) Estimation of the SLA following the methodology proposed by WMO. Basemap: Sentinel 2 MSI Imagery.

Subsequently to obtain the SCR, an algorithm based on the Otsu threshold value method was applied for image differentiation and segmentation from the frequency histogram of surface reflectance (Fig. 2). This approach was selected on the basis of its simplicity and accuracy in differentiating between two distinct classes of pixels (Otsu, 1979). Here, the segmentation was performed first on the NIR band (Rastner et al., 2019) and also on the band ratio between the NIR and SWIR established by Li et al., (2022):

$$NIRSWIR = NIR \times \left(\frac{NIR}{SWIR}\right) \quad (1)$$

where $NIRSWIR$ = new band, product of a band ratio
NIR = Near infrared band
$SWIR$ = short wavelength infrared band

It should be noted that this selection was made for the purpose of facilitating a comparison between the two snow/ice differentiations. In this regard, it is important to acknowledge that the NIR/SWIR band ratio was employed by Li et al. (2022) as a means of discriminating between snow patches situated below the SLA, thereby enabling a more accurate classification between snow and ice pixels. Similarly, the NIRSWIR band ratio exhibits a spatial resolution of 30 metres, analogous to that observed in the NIR and SWIR bands.

To acquire the SLA height of each glacier in the period of study an intersection was created between the estimated "snow zone" and elevation bands of 30 meters from the AW3D30 (Fig. 2). In the methodology proposed by the WMO, the SLA is considered as a continuous zone from where there is a snow cover greater than 50%. For this purpose, the algorithm took five consecutive elevation bands and determined if all of them met the condition. If the case is positive, the average value of the lowest elevation band is considered as the SLA, otherwise, the first elevation band is discarded and the next five are considered. The process continues successively until the appropriate SLA is found. The purpose of this procedure is to discard snow patches that are below the real snow line and that would lead to an erroneous estimation. The final result is a CSV file where the SLA calculated is stored. Furthermore, the acquisition of the SCR is based on two datasets (NIR band and NIR/SWIR band ratio), which also yield two SLAs ($SLA_{[NIR]}$ and $SLA_{[NIR/SWIR]}$).

Since we consider a valid year in which only a unique image per glacier is necessary, then we proceeded to identify outliers, i.e., SLA values that were statistically outside the normal values. For this purpose, the interquartile range (IQR) method was applied:

$$IQR = Q3 - Q1 \tag{2}$$

where $Q3$ = third quartile
$Q1$ = first quartile

In a standard way, outliers are those values that are more than 1.5 times below Q1 or above Q3, since, for a normal distribution, approximately 99.3% of the data fall within 1.5 times the IQR, meaning that values outside this range are rare and therefore probably outliers (Barbato et al., 2011). After removing outliers, we analyzed the time series trend of the $SLA_{[NIR]}$ and $SLA_{[NIR/SWIR]}$ for each glacier, and whether these were significant. This was achieved by fitting the data to a linear model and calculating the p-value.

The results were compared with three data sources: firstly, with those obtained for the Viedma, Upsala, Perito Moreno and other glaciers of the SPI by De Angelis (2014), who employed a methodology similar to ours based on a mosaic made from MODIS images of 2002 and 2004.The second and third sources used were the mass balances carried out by Popovnin et al (1999) for the years 1995/1996, 1996/1997 and 1997/1998 and those being carried out by the Inventario Nacional de Glaciares from 2015 onwards for De los Tres glacier, within the framework of glaciological monitoring. Both data sources were extracted from the World Glacier Monitoring Service - WGMS website (https://wgms.ch/data-exploration/, last visit date August 14th, 2024).

2.4 Uncertainty Estimation (u)

The estimation of the SLA uncertainty was proposed by Rastner et al. (2019) and Li et al. (2022) as the product of the root mean square error (RMSE) of three variables:

$$u = \sqrt{u_{shape}^2 + u_{DEM}^2 + u_{method}^2} \tag{3}$$
$$u = \sqrt{15^2 + 8.33^2 + 15^2} = \pm 23m$$

where u^2_{shape} = uncertainty product of the glacier contour (shapefile), which derives from the resolution of the images digitized, it is correspond to ½ pixel (15 meters).
u^2_{DEM} = vertical uncertainty of the AW3D30, based on Bettiol et al. (2021) DEM comparison study, which is 8.33 meters.
u^2_{method} = uncertainty of the SLA zonal calculation method, where the SLA is determined as the average elevation of a 30 meters elevation band, so the accuracy would be 15 meters (Li et al., 2022).

3. Results

3.1 Glaciers Snow Line Altitude Estimation

Figure 3 shows the $SLA_{[NIR]}$ and $SLA_{[NIR/SWIR]}$ time series for the four glaciers studied with their p-values. According to the algorithm, for none of the glaciers was it possible to calculate the SLA between the years 1985-1997. Unfortunately, there were no images in that time span that accomplish the conditions specified in Section 2. The Viedma glacier is the only one that shows a statistically significant trend in both cases (p[NIR] = 0.002; p[NIR/SWIR] = 0.020), the remaining three glaciers show a stationary behavior (or non-significant trend), although with a high variability

It is important to note that the use of the NIR/SWIR band ratio resulted in an increase in the height of the SLA (Fig. 3), particularly for the Viedma and Upsala glaciers and to a lesser extent for De los Tres glacier. However, the overall temporal variability is similar to that observed in the $SLA_{[NIR]}$ (Fig. 3). For the aforementioned case studies, the maximum height of the $SLA_{[NIR/SWIR]}$ reached 1707 m (Viedma, years 2015 and 2023), 1662 m (Upsala, year 2013) and 1647 m (Los Tres, year 2008). In contrast, the maximum heights of the $SLA_{[NIR]}$ reached only 1557 m, 1512 m and 1617 m respectively. A comparable pattern can be observed with regard to the minimum SLA heights (Fig. 3).

Conversely, the SLA heights of the Perito Moreno glacier yielded comparable outcomes in both instances, attaining the same maximum height (1630 m for the years 1998 and 2001). However, there are also years where the calculated height from the NIR/SWIR band ratio is demonstrably greater than that estimated with the NIR band (years 1997, 2002, 2003, 2019, 2020 and 2021, Fig. 3).

Table 2 shows the comparison between the results of De Angelis (2014), Popovnin et al (1999) and ING data with those obtained in this study. With regard to the Perito Moreno and Upsala glaciers, the $SLA_{[NIR]}$ values more closely aligned than the $SLA_{[NIR/SWIR]}$ values. In contrast, for the Viedma glacier the $SLA_{[NIR/SWIR]}$ is in close agreement with the value calculated by De Angelis (1257 m and 1260 m respectively). Nevertheless, the $SLA_{[NIR]}$ is approximately 30 metres below the previous estimates (1227 m). This discrepancy can be considered analogous to the margin of error inherent to the algorithmic process. The margin of error is ±23 m for all estimations, in accordance with the calculated uncertainty (see Equation 3).

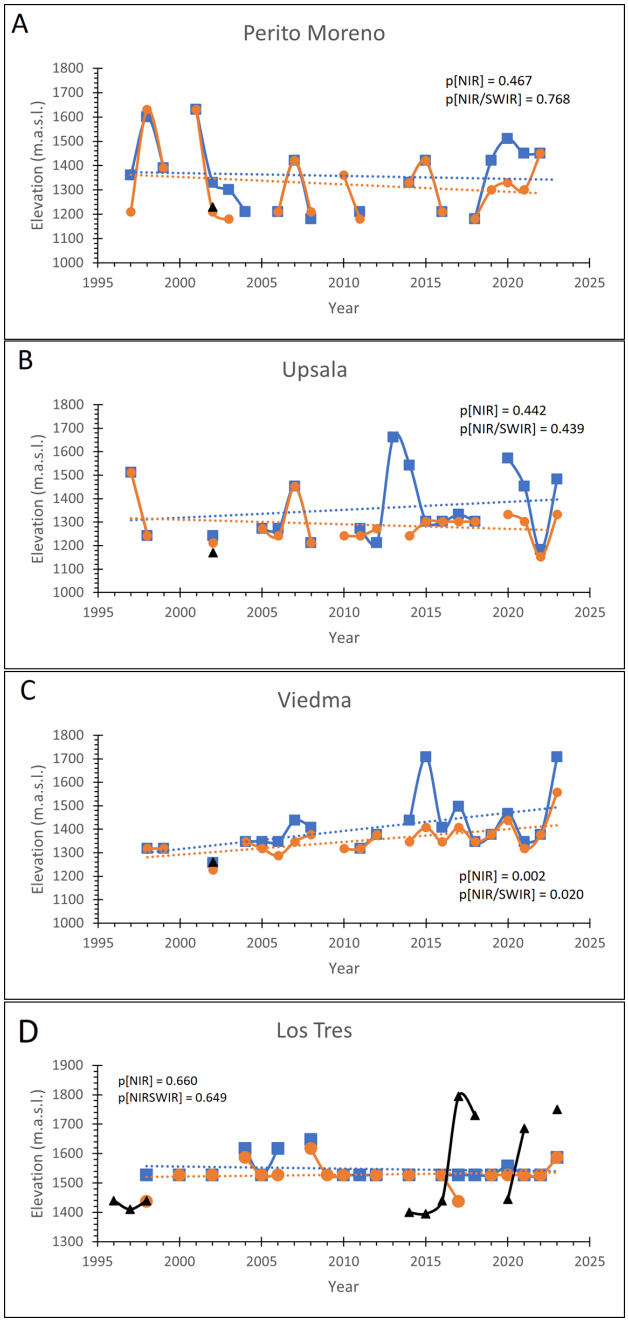

Figure 3. SLA time series changes for the 4 studied glaciers. Blue squares and orange dots represent the $SLA_{[NIR/SWIR]}$ and the $SLA_{[NIR]}$, respectively. Dashed lines represent the linear trends. *The black triangles are the SLA estimated by De Angelis for Perito Moreno (A), Upsala (B) and Viedma (C) glaciers; and also represent the ELA calculated by Popovnin and by the Inventario Nacional de Glaciares for De los Tres (D) glacier.

In contrast, the glaciological ELA ($ELA_{[glac]}$) calculated by Popovnin and colleagues for 1998 is comparable to the $SLA_{[NIR]}$, with a difference of only 3 metres. his could be regarded as a reference for the ELA at the end of the 20th century, given that the values for 1996 and 1997 are very close. However, this is not the case with the $SLA_{[NIRSWIR]}$, with which it differs by 87 metres. The differences between the $SLA_{[NIR-NIRSWIR]}$ estimates and the results obtained by the ING glaciological balances are, on the contrary, quite large. The largest difference between $ELA_{[glac]}$ and $SLA_{[NIR]}$ is 358 meters (year 2017) and the smallest is 82 meters (year 2020). A similar comparison with $SLA_{[NIRSWIR]}$ reveals a maximum difference of 268 meters (in the year 2017) and a minimum of 87 meters (in the year 2014). It is also important to highlight that the monitoring and mass balance calculations conducted by ING for the years 2017 (which exhibited the most significant discrepancy in both instances) and 2020 indicated that the entire glacier was undergoing ablation, thereby a excluding the estimation of the ELA. Nevertheless, the algorithm was able to successfully identify the $SLA_{[NIR]}$-$SLA_{[NIR/SWIR]}$ lines (Table 2), indicating that, in these cases, there would be no agreement between ELA and SLA.

It is also noteworthy that the $SLA_{[NIR]}$-$SLA_{[NIR/SWIR]}$ De los Tres glacier exhibits a singular behaviour, with practically no variation observed since 2019 (Fig. 3). This could indicate that the algorithm encounters difficulties in estimating the SLA in small glaciers, potentially due to the glacier's geometry, the challenge of identifying the Otsu threshold in small surfaces, and the presence of shadows in the selected image (Fig. 4).

Glacier	Year	$SLA_{[NIR]}$ (m)	$SLA_{[NIRSWIR]}$ (m)	SLA (De Angelis, 2014) (m)*	ELA (Popovnin et al., 1999; ING) (m)
Perito Moreno	2002	1210	1330	1230	-
Upsala	2002	1212	1242	1170	-
Viedma	2002	1227	1257	1260	-
De Los Tres	1996	-	-	-	1440
	1997	-	-	-	1410
	1998	1437	1527	-	1440
	2014	1527	1527	-	1400
	2015	-	-	-	1395
	2016	1527	1527	-	1440
	2017	1437	1527	-	1795
	2018	-	1527	-	1730
	2020	1527	1557	-	1445
	2021	1527	1527	-	1685
	2022	1527	1527	-	>2000
	2023	1587	1587	-	1750

Table 2. Comparison of the SLA values estimated in this work with that obtained by De Angelis (2014), and the ELA calculated by Popovnin et al., (1999) and by the Inventario Nacional de Glaciares. *The margin of error calculated by De Angelis, 2014 is 40 m for the Perito Moreno glacier and 30 m for the Upsala and Viedma glaciers respectively.

3.2 Additional test site: Zongo glacier (Bolivia)

In light of the limited data available for comparison in the study area and the potential causes of the near-zero variability in thein the $SLA_{[NIR-NIRSWIR]}$ time series in De los Tres glacier, it was decided to test the algorithm on a glacier that meets two criteria: (a) it has a relatively small surface area and (b) it has $ELA_{[glac]}$ data with which to make comparisons. In this context, the Zongo glacier, situated in Bolivia within the Subtropical Andes, was selected for analysis. This glacier has ELA data available from 1991 to 2021 on the WGM page. These data were produced by the French National Research Institute for Sustainable

Development (IRD) and the GREATICE team (Autin et al., 2021). The glacier has an area of 1.7 km^2.

Figure 6 shows the comparison between the SLA$_{[NIR-NIRSWIR]}$ with the ELA$_{[glac]}$ of the Zongo glacier. None of the three shows a significant trend, but a high variability. The temporal behaviour observed in the estimated SLAs and ELA$_{[glac]}$, is comparable, with years where the difference falls within the uncertainty range of the method (1993, 1998, 2005, 2017) and others with significant differences (1999, 2000, 2001, 2016). It is important to note that both the SLA$_{[NIR]}$ and the SLA$_{[NIRSWIR]}$ would be expected to overestimate the ELA. The mean difference between ELA$_{[glac]}$ and SLA$_{[NIR]}$ over the period 1991-2021 is 196 metres, while with SLA$_{[NIRSWIR]}$ is 219 meters.

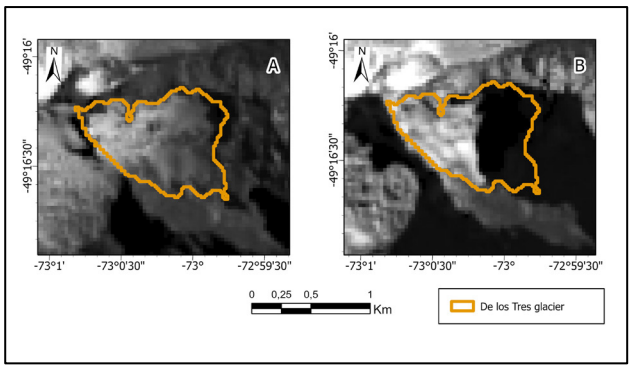

Figure 4. Two Landsat 8 images (NIR band) over the Los Tres glacier from the same year (2023), one acquired on February 5 without shadows (A) and the other acquired on April 10 with shadows (B), highlighting the possibility that the algorithm takes either image considering that there is no cloud cover in either one.

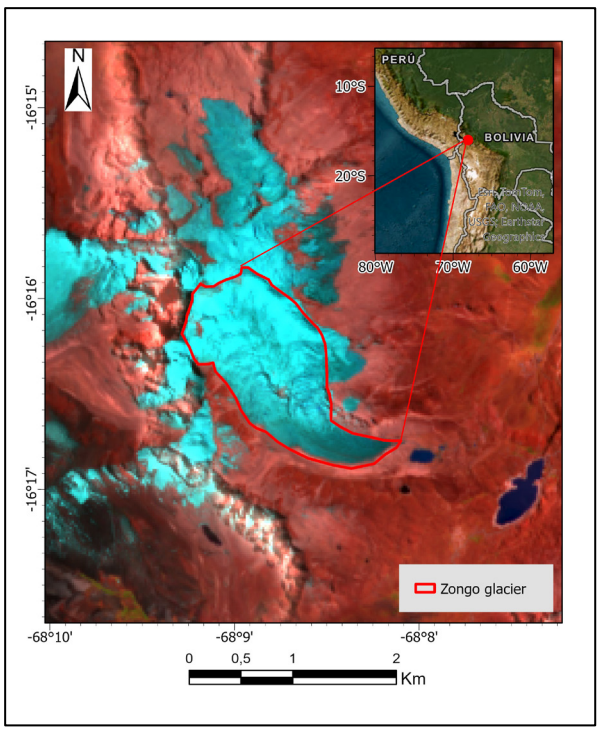

Figure 5. Figure 5. Location of Zongo glacier. Basemap: Esri, DigitalGlobe, GeoEye, Earthstar Geographics, CNES/Airbus DS, USDA, USGS, AeroGRID, IGN, and the GIS User Community; Sentinel 2 MSI Imagery.

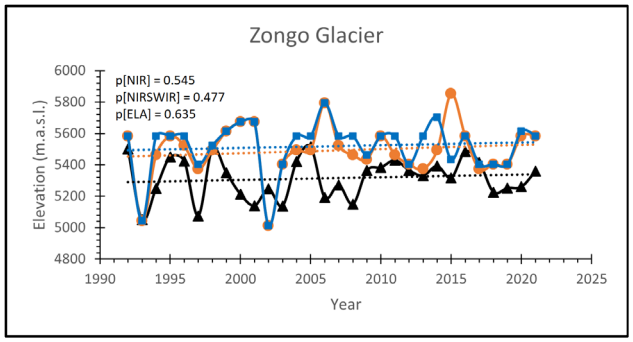

Figure 6. SLA time series changes for Zongo glacier. Blue squares and orange dots represent the SLA$_{[NIR/SWIR]}$ and the SLA$_{[NIR]}$, respectively. Dashed lines represent the linear trends. Black triangles represent the measured ELA extracted from WGMS website.

4. Conclusions

The estimated snow line altitudes for the glaciers under study demonstrate a robust tendency towards stationary, exhibiting no significant trends, with the exception of the Viedma glacier, which showed a significant positive trend indicative of an increasing SLA over time. Similarly, considering that the NIR/SWIR band ratio was taken into account due to its ability to avoid snow patches below the SLA, this also has the consequence that the SLA$_{[NIR/SWIR]}$ tends to be higher than the SLA$_{[NIR]}$ and less in agreement with the results obtained by Popovnin et al, (1999), De Angelis (2014) and the current ING glaciological monitoring. Conducting another test on the subtropical Zongo glacier, due to the unusual behavior of the estimated time series for small glaciers such as De los Tres glacier and the scarcity of data in the study area, also showed that, on average difference, there is also better agreement between ELA$_{[glac]}$ with SLA$_{[NIR]}$, although the latter as SLA$_{[NIRSWIR]}$ tend to be of higher height than ELA$_{[glac]}$. Therefore, in the future we intend to analyze these differences in depth, as well as the algorithmic difficulties inherent to the analysis of small glaciers must be considered.

References

Autin, P., Sicart, J. E., Rabatel, A., & Soruco, A. (2021). Climate controls on the interseasonal and interannual variability of the surface mass balance of a tropical glacier (Zongo Glacier, Bolivia, 16°S): New insights from the application of a distributed energy balance model over 9 years. *Earth and Space Science Open Archive*, 44. https://doi.org/10.1002/essoar.10507310.1

Bamber, J. L., Westaway, R. M., Marzeion, B., & Wouters, B. (2018). The land ice contribution to sea level during the satellite era. *Environmental Research Letters*, *13*(6), 063008. https://doi.org/10.1088/1748-9326/aac2f0

Barbato, G., Barini, E., Genta, G., & Levi, R. (2011). Features and performance of some outlier detection methods. *Journal of Applied Statistics*, *38*(10), 2133-2149. https://doi.org/10.1080/02664763.2010.545119

Bettiol, G. M., Ferreira, M. E., Motta, L. P., Cremon, É. H., & Sano, E. E. (2021). Conformity of the NASADEM_HGT and ALOS AW3D30 DEM with the Altitude from the Brazilian Geodetic Reference Stations: A Case Study from Brazilian Cerrado. *Sensors*, *21*(9). https://doi.org/10.3390/s21092935

Bown, F., Rivera, A., Pętlicki, M., Bravo, C., Oberreuter, J., & Moffat, C. (2019). Recent ice dynamics and mass balance of Jorge Montt Glacier, Southern Patagonia Icefield. *Journal of Glaciology*, *65*(253), 732-744. Cambridge Core. https://doi.org/10.1017/jog.2019.47

De Angelis, H. (2014). Hypsometry and sensitivity of the mass balance to changes in equilibrium-line altitude: The case of the Southern Patagonia Icefield. *Journal of Glaciology*, *60*(219), 14-28. https://doi.org/10.3189/2014JoG13J127

Dussaillant, I., Berthier, E., Brun, F., Masiokas, M., Hugonnet, R., Favier, V., Rabatel, A., Pitte, P., & Ruiz, L. (2019). Two decades of glacier mass loss along the Andes. *Nature Geoscience*, *12*(10), 802-808. https://doi.org/10.1038/s41561-019-0432-5

Jacob, T., Wahr, J., Pfeffer, W. T., & Swenson, S. (2012). Recent contributions of glaciers and ice caps to sea level rise. *Nature*, *482*(7386), 514-518. https://doi.org/10.1038/nature10847

Lannutti, E., Lenzano, M. G., Vacaflor, P., Rivera, A., Moragues, S., Gentile, M., & Lenzano, L. (2024). Ice thickness distribution and stability of three large freshwater calving glaciers on the eastern side of the Southern Patagonian Icefield. *Cold Regions Science and Technology*, *221*, 104158. https://doi.org/10.1016/j.coldregions.2024.104158

Lenzano, M. G., Rivera, A., Durand, M., Vacaflor, P., Carbonetti, M., Lannutti, E., Gende, M., & Lenzano, L. (2023). Detection of Crustal Uplift Deformation in Response to Glacier Wastage in Southern Patagonia. *Remote Sensing*, *15*(3), 584. https://doi.org/10.3390/rs15030584

Li, X., Wang, N., & Wu, Y. (2022). Automated Glacier Snow Line Altitude Calculation Method Using Landsat Series Images in the Google Earth Engine Platform. *Remote Sensing*, *14*(10), 2377. https://doi.org/10.3390/rs14102377

Macfee, M. W. (2023). *Spatio-temporal variability in Southern Hemisphere glacier snowline altitudes from 2000-2020*. https://etheses.whiterose.ac.uk/34177/

Meier, M. F. (1962). Proposed definitions for glacier mass budget terms. *Journal of Glaciology*, *4*(33), 252-263. https://doi.org/10.3189/S0022143000027544

Moragues, S., Lenzano, M. G., Lo Vecchio, A., Falaschi, D., & Lenzano, L. (2018). Surface velocities of Upsala glacier, Southern Patagonian Andes, estimated using cross-correlation satellite imagery: 2013-2014 period. *Andean Geology*, *45*(1), 87-103.

Mouginot, J., & Rignot, E. (2015). Ice motion of the Patagonian icefields of South America: 1984–2014. *Geophysical Research Letters*, *42*(5), 1441-1449. https://doi.org/10.1002/2014GL062661

Ohmura, A., & Boettcher, M. (2022). On the shift of glacier equilibrium line altitude (ELA) under the changing climate. *Water*, *14*(18), 2821. https://doi.org/10.3390/w14182821

Otsu, N. (1979). A threshold selection method from gray-level histograms. *IEEE transactions on systems, man, and cybernetics*, *9*(1), 62-66.

Pham-Duc, B., Nguyen, H., Phan, H., & Tran-Anh, Q. (2023). Trends and applications of google earth engine in remote sensing and earth science research: A bibliometric analysis using scopus database. *Earth Science Informatics*, *16*(3), 2355-2371.

Popovnin, V. V., Danilova, T. A., & Petrakov, D. A. (1999). A pioneer mass balance estimate for a Patagonian glacier: Glaciar De los Tres, Argentina. *Global and Planetary Change*, *22*(1-4), 255-267. https://doi.org/10.1016/S0921-8181(99)00042-9

Rastner, P., Prinz, R., Notarnicola, C., Nicholson, L., Sailer, R., Schwaizer, G., & Paul, F. (2019). On the automated mapping of snow cover on glaciers and calculation of snow line altitudes from multi-temporal landsat data. *Remote Sensing*, *11*(12), 1410. https://doi.org/10.3390/rs11121410

Rivera, A., Bown, F., Acuña, C., & Ordenes, F. (2008). Recent climate changes in western Patagonia. *Bulletin of glacier research*, *13*, 127-132.

Rivera, A., Corripio, J., Bravo, C., & Cisternas, S. (2012). Glaciar Jorge Montt (Chilean Patagonia) dynamics derived from photos obtained by fixed cameras and satellite image feature tracking. *Annals of Glaciology*, *53*(60), 147-155. https://doi.org/10.3189/2012AoG60A152

Takaku, J., Tadono, T., Doutsu, M., Ohgushi, F., & Kai, H. (2020). Updates of ‘AW3D30’ALOS global digital surface model with other open access datasets. *The International Archives of the Photogrammetry, Remote Sensing and Spatial Information Sciences*, *43*, 183-189. https://doi.org/10.5194/isprs-archives-XLIII-B4-2020-183-2020

Tamiminia, H., Salehi, B., Mahdianpari, M., Quackenbush, L., Adeli, S., & Brisco, B. (2020). Google Earth Engine for geo-big data applications: A meta-analysis and systematic review. *ISPRS journal of photogrammetry and remote sensing*, *164*, 152-170.

Zemp, M., Hoelzle, M., & Haeberli, W. (2007). Distributed modelling of the regional climatic equilibrium line altitude of glaciers in the European Alps. *Global and Planetary Change*, *56*(1-2), 83-100. https://doi.org/10.1016/j.gloplacha.2006.07.002

Zemp, M., Huss, M., Thibert, E., Eckert, N., McNabb, R., Huber, J., Barandun, M., Machguth, H., Nussbaumer, S. U., & Gärtner-Roer, I. (2019). Global glacier mass changes and their contributions to sea-level rise from 1961 to 2016. *Nature*, *568*(7752), 382-386. https://doi.org/10.1038/s41586-019-1071-0